

# Performance Comparison of Distributed IDM-STC versus Cooperative OFDM for practical Decode-and-Forward Relay-Networks

Sebastian Vorkoeper\*, Florian Lenkeit†, Volker Kuehn\*, Dirk Wübben†, Armin Dekorsy†

\* University of Rostock, Institute of Communications Engineering

Richard-Wagner-Str. 31, 18119 Rostock, Germany

Email: sebastian.vorkoeper@uni-rostock.de

† University of Bremen, Dept. of Communications Engineering

Otto-Hahn-Allee NW 1, 28359 Bremen, Germany

Email: lenkeit@ant.uni-bremen.de

**Abstract**—In this paper, we compare two different multiplexing strategies for a two-hop parallel relay channel. Precisely, we show the performance of distributed Interleave-Division-Multiplexing Space-Time Coding (dIDM-STC) and cooperative Orthogonal Frequency Division Multiplexing (cOFDM) operating in a decode-and-forward relay network, under the constraint of imperfect channel knowledge and timing and carrier frequency offsets. These impairments have to be estimated with either a complete pilot layer in dIDM-STC or orthogonal pilot symbols in cOFDM. While both schemes can cope with timing offsets of integer multiples of the sampling interval very well, cOFDM requires an adjustment of all transmit frequencies in order to avoid inter-carrier interference which would destroy orthogonality of the subcarriers and lead to severe performance degradations.

## I. INTRODUCTION

One of the major goals in wireless communications is to achieve reliable transmissions between source and destination. This is challenging, especially when source and destination are far apart from each other as the pathloss between source and destination severely degrades the transmit signal. Besides the pathloss also signal fading is critical to the overall transmission. Relay systems promise to cope with both effects simultaneously, as they allow to reduce the distances between communication nodes, which can result in an overall reduced pathloss. Also they introduce spacial diversity to the system. The latter can be exploited by having one or more relay nodes forming a virtual antenna array (VAA) and applying transmit processing known from Multiple Input Multiple Output (MIMO) systems. Different diversity techniques from classical MIMO systems can be adopted. In this paper we compare two transmit diversity techniques, one based on orthogonal and the other one on non-orthogonal medium access on the second hop, namely an Orthogonal Frequency Division Multiplexing (OFDM) based access and an Interleaved-Division-Multiplexing (IDM) based access. Since the aim is cooperation among the relays, a variation of these schemes is utilized. Here, for OFDM cooperative OFDM (cOFDM) is chosen,

This work was supported in part by the German Research Foundation (DFG) under grants KU 1221/6-1-2 and KA 841/20-2.

whereas for IDM Space-Time Coding (IDM-STC) [1] [2] is applied.

In case of cOFDM, distributed space-frequency codes (dSFC) [3], distributed cyclic delay diversity (dCDD) [4] or distributed subcarrier selection (dSCS) [5] are applicable. A major problem of cooperative OFDM is its sensitivity against carrier frequency offsets introducing intercarrier interference (ICI). Therefore, the relays have to synchronize their transmit frequencies towards the source [6] to avoid ICI. For dIDM-STC, frequency offsets are not as severe as for cOFDM since they are estimated during the multi-layer detection and subsequently compensated. The channel estimation in both systems is performed by a least-square (LS) estimator as described in [7] for dIDM-STC and [8] for cOFDM. For estimating the carrier frequency offset (CFO) in an cOFDM system, a maximum likelihood (ML) CFO estimator from [9] is implemented. As stated before, the frequency offset estimation is inherently coped with during the channel estimation in dIDM-STC.

This paper investigates the performance of cOFDM and dIDM-STC in a Decode-and-Forward (DF) two-hop multiple relay network. Here, the relays try to decode the source message and forward a re-encoded version towards the destination. The implemented Decode-and-Forward protocol does not exclude decoding errors at the relays. The performance of cOFDM and dIDM-STC applying Amplify-and-Forward (AF) protocol is discussed in [10].

In case of cOFDM, cooperation includes nonorthogonal access of the relays by Space-Frequency Coding or orthogonal access by OFDMA. As long as the subcarrier allocation in OFDMA is performed blindly without channel state information (CSI), both implementations require a low computational complexity. For dIDM-STC, the cooperation is always nonorthogonal and the layers have to be separated at the destination resulting in a higher computational complexity.

The outline of the paper is as follows: In Section II the system model and the different cooperation strategies are introduced. Wherewith, the channel model, including timing

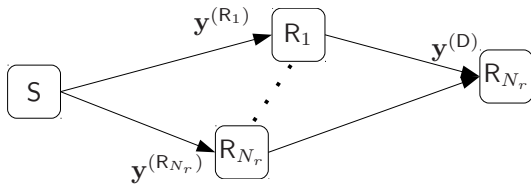


Fig. 1. Two-hop, decode-and-forward relay network

and frequency offsets are defined. Furthermore, the section delivers the description of how these offsets are estimated and compensated. Numerical results obtained by Monte-Carlo simulations are presented in Section III. The paper is closed with a summary and an outlook in Section IV.

## II. SYSTEM MODEL

The system model under investigation is depicted in **Figure 1**. The network consists of one source, multiple parallel relay nodes and a common destination. The transmission is divided into two equally long time slots  $T_1$  and  $T_2$ . In the first time slot  $T_1$ , the source  $S$  transmits its information towards the relays  $R_n$ ,  $n \in \{1 \dots N_r\}$ . During this broadcast phase each relay receives a multi-user-interference free version of the source signal. After decoding and re-encoding, the relays forward their messages during the second time slot  $T_2$  to the destination  $D$ . The channels are modeled as block fading frequency selective channels, with the corresponding channel impulse response (CIR)  $\mathbf{h}^{(s,t)}$  between transmitter  $s$  and receiver  $t$ . Furthermore, the elements of the CIR are uncorrelated and the average sum power of the channel is denoted by

$$\mathbb{E} \left\{ \|\mathbf{h}^{(s,t)}\|^2 \right\} = (a^{(s,t)})^2, \quad (1)$$

given the path loss

$$a^{(s,t)} = \sqrt{(d^{(s,t)})^{-\alpha}}, \quad (2)$$

depending on the distance  $d$  and the path loss exponent  $\alpha$ . Usually  $\alpha$  ranges from 2 to 5, i.e., free space propagation to suburban environments. During reception, the signal is disturbed by additive white Gaussian noise  $\mathbf{n}^{(t)}$ , with zero-mean and variance  $\sigma_N^2$ .

### A. Timing and frequency offsets

The time-domain receive signal  $\mathbf{y}^{(R_n)}$  at relay  $R_n$  is given by

$$\mathbf{y}^{(R_n)}[\nu] = \left( \sum_{l=0}^{L-1} h^{(S,R_n)}[l] \cdot x^{(S)}[\nu - l] \right) \cdot e^{j2\pi\epsilon_{\text{CFO}}^{(S,R_n)}\nu} + \mathbf{n}^{(R_n)}[\nu], \quad (3)$$

including the transmit signal  $\mathbf{x}^{(S)}$  of the source, the channel impulse response  $\mathbf{h}^{(S,R_n)}$  with  $L$  taps, the white Gaussian noise term  $\mathbf{n}^{(R_n)}$  and the carrier frequency offset (CFO)  $\epsilon_{\text{CFO}}^{(S,R_n)}$ , resulting from unsynchronized oscillators at source and relays, respectively. The CFO, between the source carrier

frequency  $f^{(S)}$  and the carrier frequency  $f^{(R_n)}$  of relay  $R_n$  is given by  $\epsilon_{\text{CFO}}^{(S,R_n)} = (f^{(S)} - f^{(R_n)})/f_A$ , where  $f_A$  is the sampling frequency.

Here, a timing offset between the source and the relays is not considered, as we suppose that the frame detection is perfect and the frame length is smaller than symbol timing drifts can occur. For numerical results in Section III, the frame structure is chosen to be rather simple, consisting of only one pilot OFDM symbol and a few data OFDM symbols. Thus, in this case, residual and integer frequency offsets [11] cannot be detected and, hence, only the fractional frequency offset, as the main source of intercarrier interference (ICI), is estimated. This reduces the capability of the CFO estimation to the range of  $\epsilon_{\text{CFO}}^{(s,t)} \in [-0.5, 0.5] \Delta f$ , with  $\Delta f = f_A/N_{\text{FFT}}$  as the subcarrier spacing and  $N_{\text{FFT}}$  as the number of subcarriers.

After the relays have processed their receive signals including demodulation, decoding, re-encoding, and modulation, they cooperatively forward their signals towards the destination. Since the relays are not perfectly synchronized, which would cause excessive overhead, the transmit times and frequencies slightly differ. Therefore, the resulting received signal at the destination  $D$  is given by

$$\mathbf{y}^{(D)}[\nu] = \sum_{n=1}^{N_r} \left( \left( \sum_{l=0}^{L-1} h^{(R_n,D)}[l] \cdot x^{(R_n)}[\nu + \tau_{R_n} - l] \right) \cdot e^{j2\pi\epsilon_{\text{CFO}}^{(R_n,D)}\nu} \right) + \mathbf{n}^{(D)}[\nu]. \quad (4)$$

The timing offsets between the relays are denoted as  $\tau_{R_n}$ . These offsets are caused by the relays reception and processing time, as well as the signals' traveling distances between the stations. For simplification, we assume offsets of integer multiples of the sampling interval, i.e.  $\tau_{R_n}/T_A = \tau_{R_n} \cdot f_A \in \mathbb{Z}$ .

The symbol timing offsets cause intersymbol interference at the destination. For cOFDM, the largest timing offset between to relays must be smaller than the guard interval length minus the length of the channel impulse response. Therefore,  $\tau_{R_n} \leq N_g - L$  is assumed throughout this paper, where  $N_g$  denotes the guard length. If this was not the case, cOFDM would need a more sophisticated receiver design in order to cope with the intersymbol interference.

Furthermore, carrier frequency offsets among the relays and the destination cause severe intercarrier interference. In case of cOFDM, this can not be compensated at the destination and therefore the performance of this scheme degrades.

For dIDM-STC, no such restriction are needed, as timing and frequency offsets are coped with during the multi-layer detection.

In the following subsections, an overview of the two different multiplexing strategies, i.e., cooperative Orthogonal Frequency Division Multiplexing (cOFDM) and distributed Interleave-Division-Multiplexing Space-Time Coding (dIDM-STC), is given. Here, the focus lies on operations which are performed by the source, relays and destination, as well as problems regarding complexity and advantages or disadvantages of each scheme.

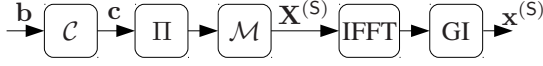


Fig. 2. Block diagram of the cOFDM source.

### B. cOFDM

In cOFDM, source, destination and relays consist of OFDM transmitter, receiver and the combination of both, respectively. The source in **Figure 2** encodes the binary input sequence  $\mathbf{b}$  with the code  $\mathcal{C}$  generating the coded sequence  $\mathbf{c}$ . This sequence is modulated with the modulator  $\mathcal{M}$  and passed through the Inverse Fast Fourier Transformation (IFFT). The size of the IFFT is given by  $N_{\text{FFT}}$ , which also reflects the number of subcarriers. Afterwards, a guard interval of length  $N_g$  is added, generating the time domain transmit sequence  $\mathbf{x}^{(S)}$ .

The relays will receive a disturbed version of the source signal denoted as  $\mathbf{y}^{(R_n)}$  and defined in (3). As depicted in **Figure 3**,  $\mathbf{y}^{(R_n)}$  is processed by the typical OFDM receiver chain including carrier frequency offset (CFO) estimation and compensation, removal of the guard interval (GI), performing the Fast Fourier Transformation (FFT) as well as channel estimation and equalization.

The carrier frequency offset estimation is performed by exploiting the guard interval, i.e. the properties of the cyclic prefix in time-domain. Therefore, a maximum likelihood (ML) estimator from [9] is implemented

$$\hat{\epsilon}_{\text{CFO}}^{(S,R_n)} = -\frac{1}{2\pi} \arg \left\{ \sum_{i=1}^{N_{\text{OFDM}}} \sum_{\mu=1}^{N_g} y_{i,\mu}^{(R_n)} \left( y_{i,\mu+N_{\text{FFT}}}^{(R_n)} \right)^* \right\}, \quad (5)$$

where  $N_{\text{OFDM}}$  denotes the OFDM symbol index. After the CFO has been compensated, the signal is transformed into frequency-domain where the channel is estimated with the help of a pilot OFDM symbol. A least-square (LS) estimator given by

$$\hat{H}_{\mu}^{(S,R_n)} = \frac{Y_{\text{Pilot},\mu}^{(R_n)}}{X_{\text{Pilot},\mu}^{(S)}} \quad (6)$$

is applied. The estimates form a diagonal channel matrix  $\hat{\mathbf{H}}^{(S,R_n)} = \text{diag} \left\{ \hat{H}_1^{(S,R_n)}, \dots, \hat{H}_{N_{\text{FFT}}}^{(S,R_n)} \right\}$ . The relays can utilize all subcarriers for channel estimation, since they all receive a complete OFDM pilot symbol from the source. Afterwards, the relays replace the pilot symbol of the source with their own pilot symbol. Since we keep the frame structure simple, only allowing one pilot symbol per hop, the relays transmit their pilot tones orthogonal on different subcarriers. Therefore, the destination has to interpolate linearly in frequency direction in order to get an estimate of the different relay-destination channels  $\hat{\mathbf{H}}^{(R_n,D)}$ .

After equalization, the resulting signal  $\tilde{\mathbf{X}}^{(S)}$  is demodulated, de-interleaved and decoded in order to get the hard decision estimate  $\tilde{\mathbf{b}}$  of the binary source sequence. This sequence is then passed through the same OFDM transmitter chain as

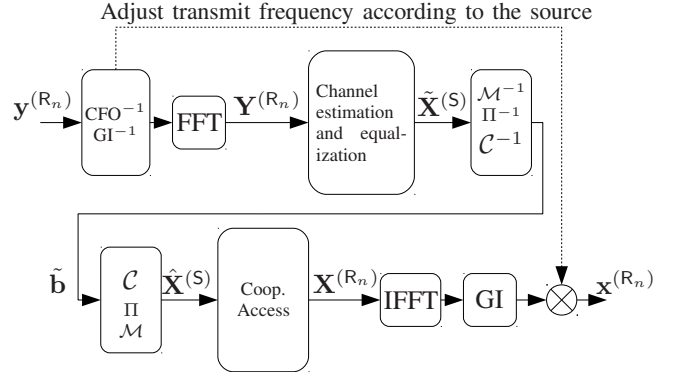


Fig. 3. cOFDM relay including the cooperative access strategy block and the transmit frequency adjustment.

for the source. The only difference being that the relays cooperatively transmit towards the destination, creating a multiple access channel on the second hop. Therefore, the relays can either apply one of different cooperation or access strategies known from multiple input single output systems or Orthogonal Frequency Division Multiple Access schemes (OFDMA). In the first case, the relays either apply distributed Space-Frequency Block-Codes (dSFBC) like Alamouti's code for  $N_r = 2$  relays or the distributed Cyclic Delay Diversity (dCDD) technique. Both techniques access the relay channel during the second time slot  $T_2$  in a non-orthogonal manner. All mentioned strategies are represented by the Coop.-Access-Block in Figure 3.

1) *Distributed Space-Frequency Block-Codes*: Since the second hop of the relay network can be seen as a Virtual Multiple Input Single Output (VMISO) system, techniques from classical MISO systems can be adopted. This includes Space-Frequency Block-Codes, which are carried out by the relays in order to achieve spatial transmit diversity. For this scheme, the destination's receiver structure can be kept simple as the decoding process is linear. One significant disadvantage, however, is the loss in code rate, if more than two relays are deployed and orthogonality is required. The only Space-Frequency Block-Code with no loss in code rate is the Alamouti code, which is applied here in case of two relays. Hence, the transmit signals of  $R_1$  and  $R_2$  in frequency-domain become

$$\mathbf{X}_{i,2\mu}^{(R_1)} = \begin{bmatrix} \hat{X}_{i,2\mu}^{(S)} \\ -(\hat{X}_{i,2\mu+1}^{(S)})^* \end{bmatrix}, \quad \mathbf{X}_{i,2\mu}^{(R_2)} = \begin{bmatrix} \hat{X}_{i,2\mu+1}^{(S)} \\ (\hat{X}_{i,2\mu}^{(S)})^* \end{bmatrix},$$

where  $\mu$  denotes the subcarrier index and  $i$  the  $i$ -th OFDM symbol. Here, multiple copies of the same sequence are transmitted by the relays in an orthogonal manner over their corresponding channels. Thus, the destination receives various replica of the same signal, combines them and therefore increases the overall probability of perfect decoding.

2) *Distributed Cyclic Delay Diversity*: In case of distributed Cyclic Delay Diversity (dCDD), the relays forward a cyclically shifted signal of the processed and re-encoded source signal. Since a cyclic shift in time-domain yields a

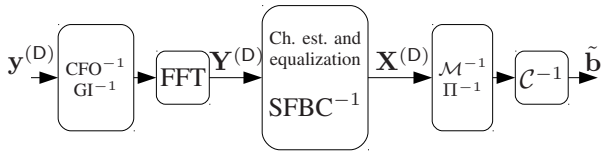


Fig. 4. cOFDM destination, including linear combining if SFBC is applied.

phase shift in frequency-domain, the resulting transmit signal at relay  $R_n$  is given by

$$X_{i,\mu}^{(R_n)} = X_{i,\mu}^{(S)} \cdot e^{-\frac{j2\pi}{N_{\text{FFT}}} \mu \delta_{R_n}}, \quad (7)$$

where  $\delta_{R_n}$  denotes the corresponding phase shift for relay  $R_n$ . The advantage of this technique is a higher diversity degree resulting from an increased effective channel impulse response length. This diversity can then be exploited by channel coding, as adjacent subcarriers are less correlated and error bursts are less likely [12].

3) *Orthogonal access by OFDMA*: For OFDMA, the available subcarriers are allocated to the relays in an orthogonal manner (distributed subcarrier selection (dSCS)). However, for the optimal subcarrier selection, all channel state information (CSI) of the second hop is needed at all relays, if the relays have to perform the subcarrier selection. Thus, a feedback of CSI from the destination to the relays is required. A second option, which slightly reduces the required overhead for the feedback, is that the destination performs the selection and only feeds back its decision towards the relays. In both cases, however, problems in form of computational complexity, signaling overhead and time variance of the channels arise. To avoid these problems and to establish a fair comparison with IDM-based techniques, no channel state information is assumed here to be exploited for the subcarrier allocation. Thus, the allocation of the subcarriers is performed only once during the setup period and fixed throughout the whole transmission. For the numerical results, a random subcarrier allocation is chosen. Furthermore, the total transmit power is constant and uniformly distributed among active subcarriers.

After the relays have applied one of the described strategies, it is mandatory to adjust the relays' transmit frequencies with respect to the transmit frequency of the source  $f^{(S)}$  [6] (see Figure 3). Otherwise, due to different relays' transmit frequencies, a Doppler spread will occur at the destination causing severe intercarrier interference, which can severely decrease the performance of OFDM based transmissions, as the orthogonality among the subcarriers is no longer preserved. The adjustment of the frequencies is performed with help of the estimated CFO  $\hat{\epsilon}_{\text{CFO}}^{(S,R_n)}$ . If all relays have perfectly measured the CFO between themselves and the source, they will transmit at the same frequency as all other relays and no intercarrier interference will occur.

The destination depicted in **Figure 4** performs the same OFDM receiver operations as the relays, including (5) and (6). Then, simple linear combining, denoted as SFBC<sup>-1</sup> in Figure

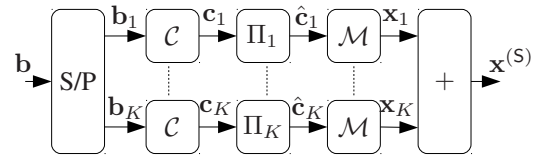


Fig. 5. IDM-STC source.

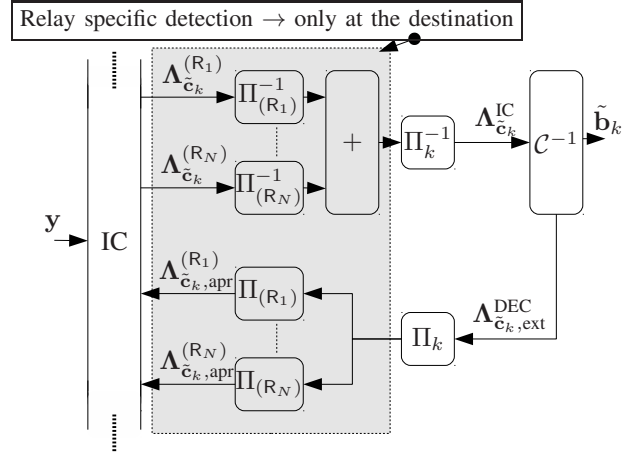


Fig. 6. Multi-layer detection (MLD) for IDM. Shown is the relevant part for layer  $k$ . At the destination, an additional relay detection and combining, i.e. decoding of the Space-Time Code, is performed (gray rectangular block).

4, is applied in case of dSFBC. Otherwise, a conventional OFDM receiver suffices for OFDMA and dCDD schemes.

### C. dIDM-STC

For dIDM-STC, the source superimposes different data layers as depicted in **Figure 5**. The binary data stream  $\mathbf{b}$  is partitioned into  $K$  data layers  $\mathbf{b}_k$ ,  $k = 1 \dots K$ . Before each layer  $\mathbf{b}_k$  is encoded and modulated with the Code  $\mathcal{C}$  and Modulator  $\mathcal{M}$ , it is interleaved with a layer-specific bit-wise interleaver  $\Pi_k$ . The resulting interleaved and modulated layers  $\mathbf{x}_k$  are superimposed in order to get the transmit signal  $\mathbf{x}^{(S)}$  of the source. Thus, the source represents a IDM transmitter.

In order to reduce the computational complexity of the IDM receiver, a soft-rake-detector is applied at the relays and the destination. For this, the iterative multi-layer detection algorithm (MLD) from [13] and [14], as depicted in **Figure 6**, has been implemented. Here, the received signal  $\mathbf{y}^{(R_n)}$  from (3) is passed into the soft-interference cancellation (IC) processor, which outputs the deinterleaved Log-Likelihood Ratios (LLRs)  $\Lambda_{\mathbf{c}_k}^{\text{IC}}$  of all layers  $k$ . Hence, all  $K$  layers are processed in parallel at the IC. The deinterleaved LLRs are fed into the decoder  $\mathcal{C}^{-1}$ , which outputs extrinsic LLRs  $\Lambda_{\mathbf{c}_k}^{\text{DEC,ext}}$  for the code bits. The extrinsic LLRs are then interleaved with the layer specific interleaver  $\Pi_k$  and passed back into the IC. Due to the iterative process, the estimates of the LLRs increase until the maximum number of iterations is reached.

The channel estimation for the dIDM-STC system is carried out following [7], i.e., by introducing an additional pilot layer  $x_p$  superimposed onto the data layers. Based on the pilot

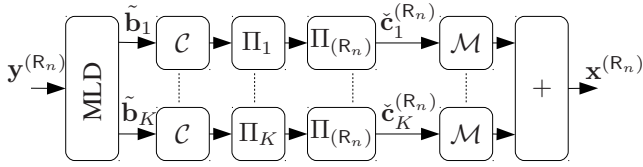


Fig. 7. IDM-STC block diagram for relay  $R_n$ .

layer and the received signal a least-squares (LS) estimation is performed. The estimate of the channel's impulse response is given as<sup>1</sup>

$$\hat{\mathbf{h}}^{(S,R_n)} = \left( \mathbf{X}_p^H \mathbf{X}_p \right)^{-1} \mathbf{X}_p^H \hat{\mathbf{y}}^{(R_n)} \quad (8)$$

where  $\mathbf{X}_p$  is the convolutional matrix of the pilot layer and  $\hat{\mathbf{y}}^{(R_n)}$  is the interference reduced received signal, i.e.,

$$\hat{\mathbf{y}}^{(R_n)} = \mathbf{y}^{(R_n)} - \hat{\mathbf{H}}^{(S,R_n)} \sum_{k=1}^K \hat{\mathbf{x}}_k. \quad (9)$$

$\hat{\mathbf{H}}^{(S,R_n)}$  and  $\hat{\mathbf{x}}_k$  are soft-estimates of the channel and the data layers, respectively, from the previous iteration. For the first iteration no previous estimates exist and, hence,

$$\hat{\mathbf{y}}^{(R_n)} = \mathbf{y}^{(R_n)} \quad (10)$$

Timing- and frequency offsets are also inherently estimated by this method as part of the channel impulse responses. Since the channel estimation is carried out for each iteration, not only the layer separation but also the channel estimation improves during the iterative detection.

After decoding, hard-decision estimates of the sources binary layers  $\tilde{\mathbf{b}}_k$  are available at each relay. This is depicted in **Figure 7**. The binary layers  $\tilde{\mathbf{b}}_k$  are re-encoded, re-interleaved with the layer-specific interleaver and additionally interleaved with a relay-specific bit-wise interleaver  $\Pi_{(R_n)}$  before modulation and superposition. Thus, taking all relays into account, a distributed multi-layer IDM-STC is created.

The destination receives  $\mathbf{y}^{(D)}$  given in (4), which is a superposition of the relays signals, i.e.  $N_r$  replica of the  $K$  data layers. Taking the channel memory  $L$  into account, in total  $K \cdot N_r \cdot L$  layers have to be separated, which is accomplished again by applying the multi-user/layer detection given in Figure 6. The relay specific replica of the same data layer are combined, i.e., the LLRs for layer  $k$  are deinterleaved and summed up<sup>2</sup>

$$\Lambda_{\tilde{\mathbf{c}}_k}^{\text{IC}} = \Pi_k^{-1} \left( \sum_{n=1}^{N_r} \Pi_{(R_n)}^{-1} \left( \Lambda_{\tilde{\mathbf{c}}_k}^{(R_n)} \right) \right), \quad (11)$$

which corresponds to the gray block in the figure. At the output of the decoder  $\mathcal{C}^{-1}$ , finally, the hard-decision estimates of the sources binary layers  $\tilde{\mathbf{b}}_k$  are available.

<sup>1</sup> $(\cdot)^H$  denotes the hermitian operation, i.e., the conjugate transposed.

<sup>2</sup>In (11),  $\Pi^{-1}$  denotes the bit-wise deinterleaver and not the product operation.

TABLE I  
SIMULATION PARAMETERS FOR THE INVESTIGATED RELAY NETWORK

Parameter	cOFDM	IDM-STC
Information bits	$N_b = 2048$	
Convolutional code	$R_c = 1/2, L_c = 3, G = [5; 7]_8$ $R_c = 1/2, L_c = 7, G = [131; 171]_8$	
Bandwidth	$BW = 20 \text{ MHz}$	
FFT size	$N_{\text{FFT}} = 512$	
CP length	$N_g = 32$	
Subcarrier spacing	$\Delta f \approx 39 \text{ kHz}$	
Repetition code		$R_r = 1/16$
Number of iterations		$N_{\text{it}} = 10$
Frame structure	1 pilot OFDM symbol 4 data OFDM symbols	1 pilot layer 8 data layer
CIR length	$L = 1, 4, 8$	
Transmit frequency	2412 MHz	
CFO S-R <sub>1</sub>	6 kHz	
CFO S-R <sub>2</sub>	-8.5 kHz	
CFO S-D	12 kHz	
Symbol timing offsets	$\tau_{R_1} = 0, \tau_{R_2} = 4$	
Normalized distance S-R <sub>1</sub>	0.51	
Normalized distance S-R <sub>2</sub>	0.51	
Normalized distance S-D	1	
Path-loss exponent	$\alpha = 3$	

### III. NUMERICAL RESULTS

In this section, we present the simulation results for dIDM-STC and cOFDM in a two-hop relay system, without direct link.

The chosen setup consists of  $N_r = 2$  relays which are placed on a two-dimensional grid at positions  $[0.5, 0.1]$  and  $[0.5, -0.1]$ . The grid is normalized such that the distance between the source at position  $[0.0, 0.0]$  and the destination at position  $[1.0, 0.0]$  amounts to  $d_{\text{SD}} = 1$ . Therefore, the distance between source and each relay is  $d_{\text{SR}_{1,2}} = 0.51$  which is included in the path-loss  $a = \sqrt{d^{-\alpha}}$  with a path-loss exponent of  $\alpha = 3$ .

The number of information bits which are transmitted from the source via the relays towards the destination is set to  $N_b = 2048$ . The bits are encoded with a non-systematic non-recursive convolutional code of rate  $R_c = 1/2$  and generator polynomials either  $G = [5; 7]_8$  or  $G = [131, 171]_8$ , with their respective constraint lengths  $L_c = 3$  and  $L_c = 7$ . Including QPSK modulation, one frame consist of  $N_s = 2048$  symbols and additional pilot symbols.

In case of cOFDM, the frame is partitioned into one complete OFDM pilot symbol and four OFDM data symbols with  $N_{\text{FFT}} = 512$  subcarriers and a guard length of  $N_g = 32$  leading to a total frame length of 2720 symbols. For the dIDM-STC System the coded information sequence is divided into  $K = 8$  data layers which are superimposed. Due to the use of a spreading code of rate  $R_r = 1/16$  each layer consists of 4096 symbols. Additionally a pilot layer of the same length is superimposed as well.

In order to achieve a fair comparison between the two different systems, the Signal-to-Noise-Ratio (SNR) is defined as the ratio of the total required transmit energy per information bit over all transmitting nodes to the noise variance, i.e.,

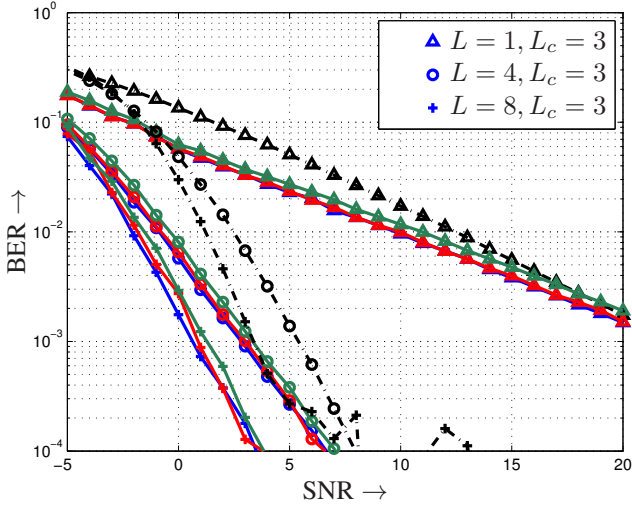


Fig. 8. BER comparison between dIDM-STC (- -, black) and cOFDM with Alamouti SFBC (-, blue), CDD (-, red) and blind dSCS (-, green). For the error correction, a convolutional code with constraint length  $L_c = 3$  is used.

$$\text{SNR} = \gamma \frac{P_{\text{tot}}/N_b}{\sigma_N^2}. \quad (12)$$

The total required energy is given as

$$P_{\text{tot}} = \frac{(1 + N_r) \cdot N_b \cdot \sigma_x^2}{\log_2(M) \cdot R}, \quad (13)$$

where  $R$  is the total code rate, i.e.,  $R = R_c$  for cOFDM and  $R = R_c \cdot R_r$  for dIDM-STC and  $\sigma_x^2$  is the power of each QPSK symbol. The required overhead for pilot symbols and guard interval is included in the SNR loss  $\gamma$  which is given as  $\gamma_{\text{OFDM}} = \frac{2048}{2720}$  for cOFDM and  $\gamma_{\text{IDM}} = \frac{8}{9}$  for dIDM-STC.

Furthermore, three different channel types are chosen for simulation, namely a flat fading channel with  $L = 1$  tap and two frequency selective channels with either  $L = 4$  or  $L = 8$  taps. The receivers do not have perfect channel state information (CSI) and they are not perfectly synchronized in terms of timing and frequency. Thus, the CSIs and the frequency offsets have to be estimated at the receivers. For simulation, a symbol timing offset of  $\tau_{R_1} = 0$  for relay  $R_1$  and  $\tau_{R_2} = 4$  for relay  $R_2$  is considered. The frequency offsets are given by  $f^{(S)} - f^{(R_1)} = 6$  kHz,  $f^{(S)} - f^{(R_2)} = -8.5$  kHz and  $f^{(S)} - f^{(D)} = 12$  kHz, respectively, where the source transmit frequency  $f^{(S)} = 2412$  MHz holds as the reference.

The comparison of cOFDM with dIDM-STC in terms of bit error rates (BER) at the destination is given in **Figure 8**. It can clearly be seen that cOFDM outperforms dIDM-STC by  $\approx 3$  dB in the lower SNR region. In this region the performance of dIDM-STC is mainly influenced by the severe multi-user-interference. While the detection for cOFDM only has to overcome the influences of the noise, the dIDM-STC detector also suffers from high interference power, corresponding to a low Signal-to-Interference-and-Noise-Ratio (SINR). Due to this low SINR, the multi-user detector often fails at properly

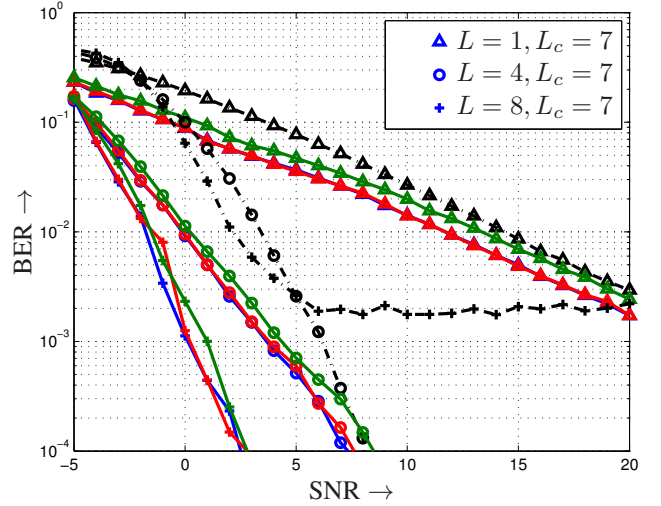


Fig. 9. BER comparison between dIDM-STC (- -, black) and cOFDM with Alamouti SFBC (-, blue), CDD (-, red) and blind dSCS (-, green). For the error correction, a convolutional code with constraint length  $L_c = 7$  is used.

separating all  $K \cdot N_r \cdot L$  layers, resulting in the observed poor performance.

As the SNR increases, the iterative multi-layer/user detection (MLD) converges to the single user bound resulting in optimal maximum ratio combining (MRC). Thereby, also the channel estimation benefits from the iterative process. This is an advantage compared to cOFDM, where the channel and frequency offset estimation is only performed once at the beginning. Although the estimation could also be enhanced with an iterative process, this was not applied here due to the higher computational complexity. Due to the weaker estimation, especially deviation of frequency offsets at the relays causes a Doppler spread at the destination. Thus, the performance of cOFDM is constrained by a good CFO estimation. Therefore, the slope of the dIDM-STC curves are steeper and the BER curves intersect with the cOFDM curves.

With additional frequency diversity from increasing channel lengths  $L$ , the decoding in the cOFDM system improves and less errors occur. The same holds for distributed IDM-STC, until the soft-rake-detection fails to separate all  $K \cdot N_r \cdot L$  layers, since their number increases linearly with the number of channel taps. The maximum number of layers the detector can separate is mainly restricted by the overall code rate  $R$  and the interleaving depth. If the number of layers exceeds the capability of the system, the layers cannot be separated and the BER will run into an error-floor as can be seen in Fig. 8 for  $L = 8$ .

For the cOFDM scheme, the BER of the different cooperation strategies are also depicted in Figure 2. Here, the distributed SFBC and CDD perform nearly the same, with a slight advantage for the dSFBC. This is due to the fact, that the Alamouti scheme achieves full spatial diversity. In case of CDD, the correlations between fading coefficients are reduced from the increasing effective channel impulse response. The

resulting higher diversity degree is then exploited by the channel decoder. Blind random distributed subcarrier selection (dSCS), finally, performs  $\approx 0.5$  dB worse than CDD. Here, the relays transmit with an increased power per subcarrier, but neither spatial diversity nor higher diversity from an increased effective channel length is utilized.

The same observations generally also hold for the results obtained for the convolutional code with constraint length  $L_c = 7$ , depicted in **Figure 9**. Due to the stronger channel code, cOFDM can fully exploit the offered frequency diversity which was not possible for the weaker code before. For dIDM-STC, on the other hand, a stronger channel code leads to a worse performance. The reason for this behaviour is due to the better performance of the weaker code in the very low SNR region. Since the overall interference is very high at the beginning of the iterative detection, here, the weaker code results in a better behaviour of the overall detection.

#### IV. CONCLUSION

In this paper, the performance of cooperative OFDM and distributed IDM-STC is analyzed under the constraint of imperfect channel knowledge and carrier frequency offsets (CFO), as well as timing offsets.

For both schemes, integer multiples of the sampling interval in a certain range will not decrease the performance. Furthermore, it was shown that for cOFDM the relays need to adjust their transmit frequencies according to the source, otherwise intercarrier-interference will occur at the destination. This strongly depends on the CFO estimation on the first hop. In case of dIDM-STC, no such operation is needed as the CFO is inherently estimated and compensated during the multi-layer/user detection. The main drawback of dIDM-STC is the dependency of the detection success on the number of overall layers. With increasing number of channel taps also the number of layers increases. After the system's capability is reached the iterative detection fails. In order to cope with this problem other detection strategies, e.g., based on MMSE-detection could be applied. Also a combination of OFDM with IDM-STC as shown in [15] and [16] should be considered.

#### REFERENCES

[1] Z. Fang, L. Li, and Z. Wang, "An Interleaver-Based Asynchronous Cooperative Diversity Scheme for Wireless Relay Networks," in *IEEE International Conference on Communications*, Beijing, China, May 2008.

[2] P. Weitkemper, D. Wübben, and K.-D. Kammeyer, "Distributed Interleave-Division Multiplexing Space-Time Codes for Coded Relay Networks," in *Sixth International Symposium on Wireless Communication Systems*, Siena, Italy, Sept. 2009.

[3] Tsung-Ta Lu, Hsin-De Lin, and Tzu-Hsien Sang, "An SFBC-OFDM receiver to combat multiple carrier frequency offsets in cooperative communications," in *Proc. IEEE 21st Int Personal Indoor and Mobile Radio Communications (PIMRC) Symp*, 2010, pp. 899–904.

[4] S. Ben Slimane and A. Osseiran, "Relay Communication with Delay Diversity for Future Communication Systems," in *Proc. VTC-2006 Fall Vehicular Technology Conf. 2006 IEEE 64th*, 2006, pp. 1–5.

[5] Yuwen Pan, A. Nix, and M. Beach, "Distributed Resource Allocation for OFDMA-Based Relay Networks," vol. 60, no. 3, pp. 919–931, 2011.

[6] Oh-Soon Shin, A. M. Chan, H. T. Kung, and V. Tarokh, "Design of an OFDM Cooperative Space-Time Diversity System," vol. 56, no. 4, pp. 2203–2215, 2007.

[7] Hendrik Schoeneich and Peter Adam Hoehner, "Iterative Pilot-Layer Aided Channel Estimation with Emphasis on Interleave-Division Multiple Access Systems," *EURASIP J. Adv. Sig. Proc.*, vol. 2006, 2006.

[8] J.-J. van de Beek, O. Edfors, M. Sandell, S. K. Wilson, and P. O. Borjesson, "On channel estimation in OFDM systems," in *Proc. IEEE 45th Vehicular Technology Conf*, 1995, vol. 2, pp. 815–819.

[9] J. J. van de Beek, M. Sandell, and P. O. Borjesson, "ML estimation of time and frequency offset in OFDM systems," vol. 45, no. 7, pp. 1800–1805, 1997.

[10] P. Weitkemper, S. Vorköper, D. Wübben, K.-D. Kammeyer, and V. Kühn, "Distributed IDM-STC versus OFDM-CDD in Two-Hop Relay-Networks," in *14th International OFDM-Workshop (InOWo 2009)*, Hamburg, Germany, september 2009.

[11] Qi Wang, C. Mehlführer, and M. Rupp, "Carrier frequency synchronization in the downlink of 3GPP LTE," in *Proc. IEEE 21st Int Personal Indoor and Mobile Radio Communications (PIMRC) Symp*, 2010, pp. 939–944.

[12] G. Auer, "Channel estimation for OFDM with cyclic delay diversity," in *Proc. 15th IEEE Int. Symp. Personal, Indoor and Mobile Radio Communications PIMRC 2004*, 2004, vol. 3, pp. 1792–1796.

[13] W.K. Leung, K.Y. Wu, and Li Ping, "Interleave-Division-Multiplexing Space-Time Codes," *IEEE Vehicular Technology Conference (VTC-Spring 2003)*, vol. 2, pp. 1094–1098, Oct. 2003.

[14] L. Ping, L. Liu, K.Y. Wu, and W.K. Leung, "Interleave-Division Multiple-Access," *IEEE Transactions on Wireless Communications*, vol. 5, no. 4, pp. 938–947, Apr. 2006.

[15] P. Weitkemper and G. Bauch, "Distributed interleave-division-multiplexing space-frequency-codes," in *Proc. 8th Int Multi-Carrier Systems & Solutions (MC-SS) Workshop*, 2011, pp. 1–5.

[16] F. Lenkeit, C. Bockelmann, D. Wübben, and A. Dekorsy, "OFDM-IDM Space-Time Coding in Two-Hop Relay-Systems with Error-Prone Relays," in *International ITG Workshop on Smart Antennas (WSA'12)*, Dresden, Germany, march 2012.